
TRANSFORMER-BASED ASSIGNMENT DECISION NETWORK FOR MULTIPLE OBJECT TRACKING

PREPRINT

✉ **Athena Psalta**

Remote Sensing Laboratory
National Technical University of Athens
Iroon Polytechniou 9, Athens 15780, Greece
psaltaath@central.ntua.gr

✉ **Vasileios Tsironis**

Remote Sensing Laboratory
National Technical University of Athens
Iroon Polytechniou 9, Athens 15780, Greece
tsironisbi@central.ntua.gr

✉ **Konstantinos Karantzas**

Remote Sensing Laboratory
National Technical University of Athens
Iroon Polytechniou 9, Athens 15780, Greece
karank@central.ntua.gr

ABSTRACT

Data association is a crucial component for any multiple object tracking (MOT) method that follows the tracking-by-detection paradigm. To generate complete trajectories such methods employ a data association process to establish assignments between detections and existing targets during each timestep. Recent data association approaches try to either solve a multi-dimensional linear assignment task or a network flow minimization problem or tackle it via multiple hypotheses tracking. However, during inference an optimization step that computes optimal assignments is required for every sequence frame inducing additional complexity to any given solution. To this end, in the context of this work we introduce Transformer-based Assignment Decision Network (TADN) that tackles data association without the need of any explicit optimization during inference. In particular, TADN can directly infer assignment pairs between detections and active targets in a single forward pass of the network. We have integrated TADN in a rather simple MOT framework, we designed a novel training strategy for efficient end-to-end training and demonstrate the high potential of our approach for online visual tracking-by-detection MOT on two popular benchmarks, i.e. MOT17 and UA-DETRAC. Our proposed approach demonstrates strong performance in most evaluation metrics despite its simple nature as a tracker lacking significant auxiliary components such as occlusion handling or re-identification. The implementation of our method is publicly available at <https://github.com/psaltaath/tadn-mot>

Keywords Visual Object Tracking · Data Association · Tracking-by-Detection · MOT17 · UA-DETRAC

1 Introduction

Multiple object tracking (MOT) aims at identifying objects of interest in a video sequence and representing them as a set of trajectories through time. In recent years, MOT has drawn significant attention due to its critical role in a wide range of applications such as traffic surveillance (Tian et al. [2019]), autonomous driving (Chen et al. [2017a], Osep et al. [2017]) and human behavior prediction (Psalta et al. [2020]).

Due to recent advancements in object detection, most modern trackers (Tian et al. [2018] Bergmann et al. [2019]) follow a tracking-by-detection pipeline where objects of interest localized by a detector are associated by a predefined metric in order to form existing trajectories. Missing detections, interaction between targets in a crowded scene and partial/full occlusions of targets are only few of the challenges that MOT algorithms struggle with and can often lead to trajectory

fragmentation and low performance. Under an online context, tracking-by-detection approaches rely heavily on data association methods in order to compose target trajectories through comparing detection hypotheses only with existing trajectories within a video frame.

In most existing methods, this data association process relies on computing a set of similarity scores between existing trajectories and detections. In general, a significant number of modern MOT algorithms rely heavily on data association methods such as network flow optimization like Dehghan et al. [2015] or the Hungarian algorithm (Kuhn [1955]). However, in any case a final optimization step is always required in order to infer the optimal assignments between multiple detections and existing targets adding extra complexity to a typical MOT algorithm.

In this work, we have designed and developed a data-driven method that offers an alternative approach to the data association task. In particular, we leveraged the Transformer architecture, introduced in Vaswani et al. [2017], to formulate an assignment decision network, named Transformer-based Assignment Decision Network (TADN), that eliminates the need for explicitly solving a Linear Data Association Problem (LDAP) during the inference stage. Our work is further motivated by the fact that most LDAP solvers such as the Hungarian algorithm are not differentiable, except a few approaches such as Xu et al. [2020], thus hindering an end-to-end trainable MOT tracker formulation. Moreover, we discuss the actual contribution of data association in a tracking-by-detection scheme offering several experiments and valuable ablations. Furthermore, in order to demonstrate the effectiveness of our method, we built an online MOT algorithm that integrates the novel data association method. We conducted experiments on challenging MOT benchmarks such as MOT17 (Milan et al. [2016], Dendorfer et al. [2021]) and UA-DETRAC (Wen et al. [2020]); our results showed strong, superior even, performance against well known methods varying by their data association approach, even without incorporating any occlusion handling or re-identification components as many of the compared methods do. Our contributions are summarized as follows:

- We introduce a novel data association method, named TADN, for visual, online MOT without solving explicitly a LDAP during inference.
- We provide a baseline tracking-by-detection implementation along with the source code that integrates TADN coupled with simple submodules for motion and appearance modeling.
- We offer an extensive experimental validation in challenging MOT benchmarks that demonstrate the superior performance of TADN against methods employing alternative data association methods.

This paper is structured as follows : Section 2 contains a review of the related literature regarding data association methods for multiple object tracking and Transformer architectures. In Section 3 we introduce our novel method for data association, while describing also the implemented tracking algorithm. In Section 4 we submit the results of our approach on two challenging benchmarks along with a detailed ablation study for our method. Last, in Section 5 a series of conclusions and limitations are drawn along with some further future extensions are discussed.

2 Related Work

Data association in MOT. Recent advances of object detection methods (Ren et al. [2015], Yang et al. [2016a]) have established tracking-by-detection as a common paradigm for multiple object tracking. Based on the detected objects of interest the goal is to associate them through time in order to form target trajectories. This association process is basically a joint optimization problem where information about newly observed objects such as their position or appearance is compared to relevant information about active targets in the current frame.

Data association can be performed offline (batch-mode) by exploiting information both from past and future trajectories (Tang et al. [2016]). However, the rise of real-time applications have established online methods that exploit only information from past trajectories as the most popular over the years (Bergmann et al. [2019], Zhang et al. [2021]). Under an online context, the assignment problem can be formulated as a LDAP optimization problem between two consecutive frames and is solved by bipartite matching algorithms such as the Hungarian algorithm (Bewley et al. [2016], Fang et al. [2018]). Building upon that concept, Deep Affinity Network (DAN) introduced by Sun et al. [2019] models both appearance and affinity between objects over time producing a soft assignment matrix and applies the Hungarian algorithm to predict the optimal assignments in a supervised manner using ground truth assignment matrices. Similarly, Chu and Ling [2019] expand on the idea of affinity estimation by directly learning to predict the correct assignments. Moreover, DeepMOT (Xu et al. [2020]) introduces an end-to-end training framework that uses differentiable versions of MOTA and MOTP (Bernardin and Stiefelhagen [2008]) evaluation metrics as loss function and proposes the Deep Hungarian Network (DHN) as a linear assignment method between detection hypotheses and active trajectories.

Alternative data association methods apply under the multiple hypotheses tracking (MHT) scheme, such as Reid [1979], where a trade-off between maintaining and removing hypotheses with high and low confidences respectively

is considered. In this case the assignment problem is formulated as a maximum weighted independent set (MWIS) problem. Due to the exponential growth of hypotheses, recent works such as Chen et al. [2017b] introduce an enhancing detection model to cope with data association ambiguities, while Sheng et al. [2018a] propose a tracklet-level association pruning methods and approximation algorithms for the MWIS problem.

In addition, a significant number of alternative data association approaches rely on network flow-based (Dehghan et al. [2015], Wang et al. [2015]) or graph matching (He et al. [2021]) methods where the total sum of pairwise costs is minimized. These assignment costs can either be based on heuristics or even be learnable. Schulter et al. [2017] introduce an end-to-end trainable pipeline for network-flow formulations where a set of arbitrary parameterized cost functions are learned. Tang et al. [2017] propose a minimum cost lifted multicut problem as a way to jointly cluster detections hypotheses over time. Also, Sheng et al. [2018b] introduce a heterogeneous association fusion (HAF) tracker to deal with detection failures and considers a multiple hypotheses formulation for the assignment problem. Other approaches use reinforcement learning techniques for data association, such as the work from Xiang et al. [2015], where a target trajectory is initialized, terminated or maintained regarding a learnable policy over a Markov decision process.

All in all, most of the approaches discussed above rely on the computation of a cost matrix to explicitly solve a linear data association problem (LDAP). In general, such an approach introduces a computational overhead to a MOT algorithm that varies given the number of detections and targets in a scene. Thus, this process occupies a significant portion of the available computational budget for real time applications. Multiple hypotheses techniques have in principle high computational complexity, while network flow and graph-based data association methods need to enforce global optimization on large graphs constraining their potential for real-time MOT. Our method follows the tracking-by-detection paradigm and is based to an assignment decision network that does not need to solve a LDAP problem during inference time.

Transformer architectures. Since their first appearance in natural language processing (Vaswani et al. [2017]), Transformers have achieved significant success in a plethora of computer vision applications, such as person re-identification (Liu et al. [2019]) and object detection (Carion et al. [2020]). Recent works have investigated the success of these architectures in MOT. Meinhardt et al. [2022] set up a joint detection and tracking pipeline modifying the object detector DETR (Carion et al. [2020]) to an end-to-end MOT algorithm through propagating queries over time. In a similar manner, MOTR Zeng et al. [2022] formulate MOT as a problem of "set of sequence" predictions and also builds upon DETR (Carion et al. [2020]) extending its object queries to "track queries" to predict object sequences. TransMOT introduced by Chu et al. [2021] treats target trajectories as a set of sparse weighted graphs and models their interactions through temporal and spatial transformer encoder and decoder layers respectively. Furthermore, TrackFormer (Meinhardt et al. [2022]) introduces a tracking-by-attention approach where detection and data association are jointly achieved and leverages a Transformer architecture where the encoder extracts CNN features for each frame and the decoder produces query embeddings with identified bounding boxes. TransCenter (Xu et al. [2021]) handles detection related problems in tracking, such as missing detections or very dense detections in overlapping anchors, proposing dense detection queries, as well as introduces sparse tracking queries to overcome computational efficiency problems related to the quadratic complexity nature of Transformers.

In order to exploit the capacity of these architectures, in this work we introduce a novel data association method based on a Transformer architecture showing strong performance on popular MOT benchmarks. Our intuition is based on the insight that these architectures leverage self-attention and cross-attention mechanisms to model the relationships between the encoder and decoder inputs, that in our case are mapped to detection boxes and existing trajectories in the scene respectively.

3 Methodology

We designed and implemented Transformer-based Assignment Detection Network (TADN) as an alternative to data association for MOT. In short, TADN transforms information related to detections and known targets in each frame to directly compute optimal assignments for each detection. To evaluate TADN’s real-world performance, a simple tracking-by-detection MOT algorithm was implemented to support it. Our tracker, including TADN, was end-to-end trained via the proposed novel training strategy.

3.1 Transformer-based Assignment Detection Network

TADN operates on every time-step to condition two separate input data streams using a series of self- and cross-attention mechanisms. Let $D_{in} \in \mathbb{R}^{N \times F_D}$ be the set of N detections in each frame while $T_{in} \in \mathbb{R}^{M \times F_T}$ be the set of M previously tracked targets. In either stream, information from multiple cues is incorporated into a set of vectors via

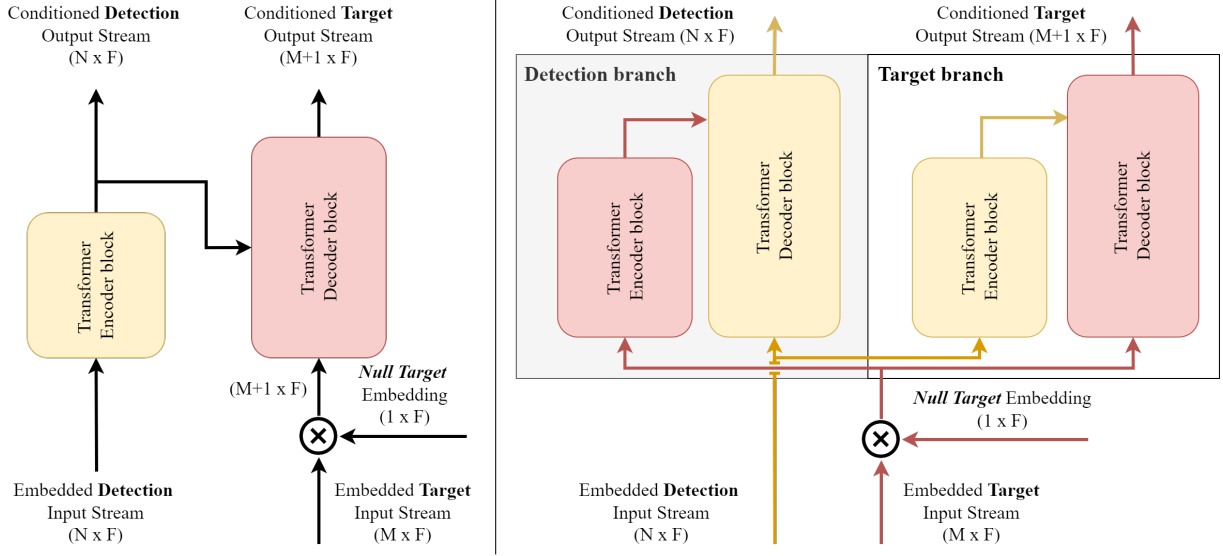


Figure 1: **Single and dual branch configurations for TADN.** **Left:** Single branch approach is constituted of a single Transformer model. Target and Detection input streams are fed to the decoder and encoder part respectively. Target output stream is the Transformer’s standard output, while Detection output stream the output of the Transformer’s encoder. **Right:** Dual branch version uses two separate Transformer models. Each output stream corresponds to the output of each Transformer model. Detection and Target input stream are fed to the decoder and encoder part respectively for the Detection branch and vice-versa for the Target branch. In both architectures, a *null target* embedding is concatenated to the Target input stream before feeding it to the Transformer.

linear embedding layers L_D, L_T of dimension d_{model} producing $D'_{in} \in \mathbb{R}^{N \times d_{model}}$ and $T'_{in} \in \mathbb{R}^{M \times d_{model}}$ as shown in Equation 1.

$$\begin{aligned} D'_{in} &= L_D(D_{in}) \in \mathbb{R}^{N \times d_{model}} \\ T'_{in} &= L_T(T_{in}) \in \mathbb{R}^{M \times d_{model}} \end{aligned} \quad (1)$$

The final output of the TADN module is two sets of vectors. Let $D_{out} \in \mathbb{R}^{N \times d_{model}}$ and $T_{out} \in \mathbb{R}^{M \times d_{model}}$ be the set of output transformed feature vectors related to detections and actively tracked targets respectively:

$$D_{out}, T_{out} = TADN(D'_{in}, T'_{in}; \theta_{TADN}) \quad (2)$$

where θ_{TADN} the set of TADN’s architecture parameters.

It should be noted that T_{out} has one more vector compared to the corresponding input set T_{in} to compensate for the case of not assigning a detection to a specific target. This extra target is identified as the *null target* and a corresponding learnable embedding vector $T_{null} \in \mathbb{R}^{d_{model}}$ is concatenated to T'_{in} . In that way, Equation 1 is adjusted as:

$$\begin{aligned} D'_{in} &= L_D(D_{in}) \in \mathbb{R}^{N \times d_{model}} \\ T'_{in} &= L_T(T_{in}) \oplus T_{null} \in \mathbb{R}^{M+1 \times d_{model}} \end{aligned} \quad (3)$$

where \oplus denotes the concatenation operator.

To derive the final assignments, first the *Assignment Score Matrix (ASM)* is computed as the scaled dot product between the two output sets:

$$ASM_{N \times M+1} = \frac{D_{out} T_{out}^T}{\sqrt{d_{model}}} \quad (4)$$

Final assignments A_{final} are computed as the $argmax$ of each row of the ASM as shown in Equation 5. Assigning a detection to the last column of ASM corresponds to an assignment to the *null target* i.e. a non-assignment.

$$A_{final} = \mathbf{argmax}(ASM, dim = 1) \in \mathbb{I}^N \quad (5)$$

where $\mathbb{I} = \{1, \dots, M + 1\} \subset \mathbb{N}$

In detail, TADN exploits the set-to-set nature of Transformers. In fact, two different architecture configurations have been designed for TADN; a *single TADN_{single}* and a *dual TADN_{dual}* branch version as shown in Figure 1.

Regarding *TADN_{single}* (Figure 1, Left), D'_{in} and T'_{in} are fed directly into the encoder and decoder part respectively of a typical Transformer model introduced by Vaswani et al. [2017]. T_{out} and D_{out} are mapped to the outputs of the decoder and encoder parts of the Transformer respectively.

$$\begin{aligned} D_{out} &= \mathbf{Enc}(D'_{in}; \theta_{enc}) \\ T_{out} &= \mathbf{Dec}(T'_{in}, D_{out}; \theta_{dec}) \end{aligned} \quad (6)$$

where \mathbf{Enc} and \mathbf{Dec} are the Encoder and Decoder parts of a typical Transformer architecture with θ_{enc} and θ_{dec} parameters respectively.

Here, D_{out} is solely dependent on the D'_{in} since the encoder part of the transformer is comprised only from self-attention layers, while T_{out} is jointly dependent on both D'_{in} and T'_{in} since apart from the self-attention layers, the decoder part has one cross-attention layer for each decoder layer. Our main intuition is that T_{out} contains information about the active targets transformed by taking also into consideration the detections found in the next frame of the sequence. On the other hand, D_{out} contains information directly derived from D'_{in} transformed in order to be useful in the cross-attention layer of the decoder.

For *TADN_{dual}*, two separate Transformer models are used (Figure 1, Right). Each Transformer outputs either D_{out} or T_{out} . In the *detection branch* T'_{in} is fed in the encoder while D'_{in} in the decoder of the Transformer to derive D_{out} and vice-versa for the *target branch* to derive T_{out} :

$$\begin{aligned} D_{out} &= \mathbf{Transformer}_D(T'_{in}, D'_{in}; \theta_D) \\ T_{out} &= \mathbf{Transformer}_T(D'_{in}, T'_{in}; \theta_T) \end{aligned} \quad (7)$$

where $\mathbf{Transformer}_D$ and $\mathbf{Transformer}_T$ are the Transformer models for *detection* and *target* branch with parameters θ_D and θ_T respectively.

In that case, all known targets attend to all detections in either branch. *TADN_{dual}* requires essentially double learnable parameters and computations than *TADN_{single}*. By intuition *TADN_{dual}* has higher capacity than *TADN_{single}* since both T_{out} and D_{out} are dependent on T'_{in} and D'_{in} as cross-attention layers are found in either branch, whereas in the *single branch* version only T_{out} is conditioned on both inputs.

3.2 Tracking-by-detection with TADN

To demonstrate our method’s performance we opted for a tracking-by-detection scheme featuring only an appearance model and a motion model to generate representations for detections and targets (Figure 2). As an appearance model we chose to retain raw CNN features for the last assignment on a patch-level from a ResNet50 (He et al. [2016]) architecture pretrained on a re-identification downstream task, as described in Bergmann et al. [2019]. As a motion model we opted for the standard Kalman filter (Kalman [1960]) paired with Enhanced Correlation Coefficient (ECC) based motion compensation introduced by Evangelidis and Psarakis [2008]. No further specialized modules such as re-identification (Re-ID) or occlusion handling have been included in our tracking algorithm. We opted for such a basic configuration to remove any bias/gains induced from using more specialized components. Doing so, we validated the performance impact of TADN in an unbiased way.

As described in Algorithm 1, our MOT pipeline leverages information generated from each incoming frame along with information regarding actively tracked targets already known from previous steps. More specifically, using a pretrained object detector box locations are derived for the objects in the scene. For each detected object, its corresponding image patch is extracted and CNN features are computed. These appearance and positional features are concatenated into D_{in} . Similarly, for each active target its positional and appearance features are concatenated also into T_{in} . Subsequently, D_{in} and T_{in} are fed to TADN which outputs ASM . Final assignments are derived using Equation 5.

To enable complete tracking functionality, we opted for a set of heuristic rules regarding post-association steps such as target update, spawn and termination (Algorithm 2). Initially, given that TADN outputs one assigned target (including

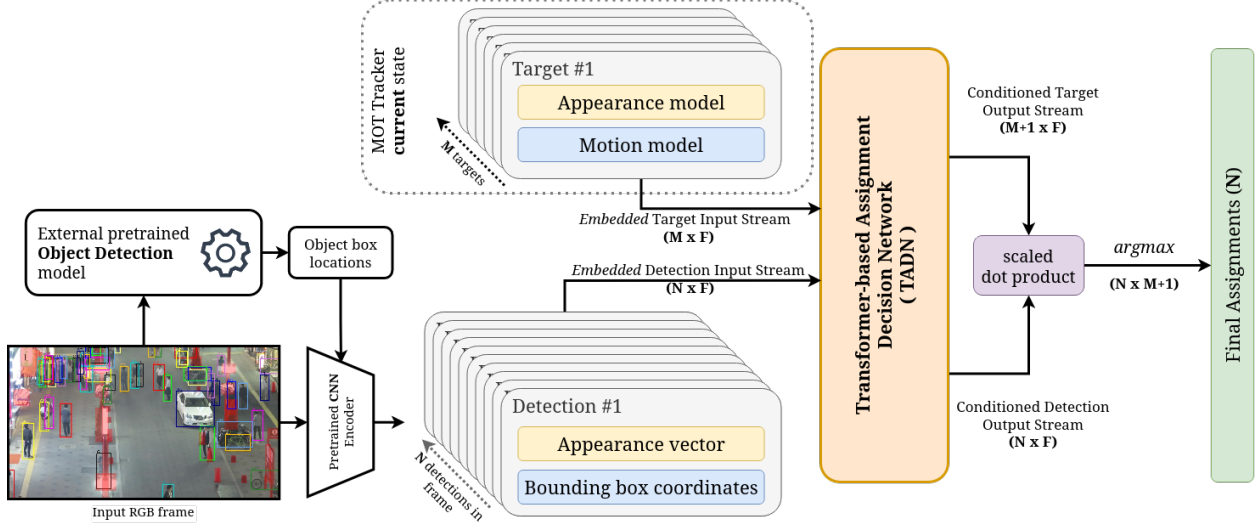


Figure 2: **Overview of our MOT pipeline.** Two input streams containing positional and appearance information are generated for N detections and M currently active targets respectively. These are fed to TADN to compute an $(N \times M + 1)$ similarity. Final assignments are directly computed via a row-wise *argmax* operation. The final assignments include the *null target* case.

Algorithm 1 Compute assignments

Input: Tracker state: motion models $\{MM_i\}_{i=1}^M$
Tracker state: appearance models $\{AM_i\}_{i=1}^M$,
Image frame $\mathbf{I} \in \mathbb{R}^{H \times W \times 3}$,
Detection locations $\{BB_i\}_{i=1}^N$, $BB_i \in \mathbb{R}^4$,
CNN feature extractor $\mathbf{F} : \mathbb{R}^{H \times W \times 3} \rightarrow \mathbb{R}^{d_F}$

Output: Final assignments for frame \mathbf{I}

Compute D_{in} :

- 1: $D_{in} \leftarrow \emptyset$
- 2: **for** each detection $i = 1, \dots, N$ **do**
- 3: Get location $BB_i = (x_i, y_i, w_i, h_i)$
- 4: Crop patch $P_i \leftarrow \mathbf{I}(BB_i)$
- 5: Compute appearance features
 $A_i^D \leftarrow \mathbf{F}(P_i)$
- 6: Update $D_{in} \leftarrow D_{in} \cup \{L_D(A_i^D \oplus BB_i)\}$
- 7: **end for**

Compute T_{in} :

- 8: $T_{in} \leftarrow \emptyset$
- 9: **for** each target $j = 1, \dots, M$ **do**
- 10: Predict location $BB_j \leftarrow MM_j.predict()$
- 11: Retrieve appearance features
 $A_j^T \leftarrow AM_j.step()$
- 12: Update $T_{in} \leftarrow T_{in} \cup \{L_T(A_j^T \oplus BB_j)\}$
- 13: **end for**

Compute assignments :

- 14: $D_{out}, T_{out} \leftarrow \mathbf{TADN}(T_{in}, D_{in}; \theta_{TADN})$
- 15: Compute ASM as in Equation 4
- 16: $A_{final} \leftarrow \mathbf{argmax}(ASM, dim = 1)$

17: **return** A_{final}

the *null target*) per detection, we filter-out any duplicate targets in the assignments (excluding *null target*) based on highest prediction confidence. Any filtered-out assignments are discarded. The remaining are used to update the motion and appearance models of the assigned targets. Next, the target termination step is performed; any targets that haven't been assigned to any detection for T_h past consecutive frames are set to an inactive state and their trajectory is considered final. However, having a constant threshold T_h is problematic since we need to terminate early those trajectories with very few "hits", i.e. total detections assigned to target since its creation. On the other hand, we can rely more on the motion model trajectory predictions for targets that have a long history, thus we opted for a variable T_h as a function of the total number of "hits" per target. We used a sigmoid function that smoothly transitions from T_h^{min} to T_h^{max} as number of "hits" rises from 0 to H_{max} :

$$t_\delta = T_h^{max} - T_h^{min}$$

$$T_{h_i} = t_\delta \cdot \sigma\left(15 \left(\frac{h_i}{H_{max} - 0.5}\right)\right) + T_h^{min} \quad (8)$$

where σ is the sigmoid function, h_i the total number of hits for target i .

Finally, new targets are spawn given all *null target*-assigned detections. For each such detection a new tracklet is created by initializing its motion and appearance models using the corresponding box locations and CNN features.

3.3 Training strategy

To train our MOT model, we designed an end-to-end training strategy. We formulated a classification problem which is optimized for every frame and considers each detection separately. The target categories are the set of active targets plus an extra category for the *null target*. Given that the outcome of TADN, i.e. the *Assignment Score Matrix* (*ASM*) is a matrix of shape $(N \times M + 1)$, it is straightforward to serve as the "logits" output for the classification problem.

To define a categorical cross-entropy loss function over these outcomes a target one-hot encoded (row-wise) matrix of similar shape was formulated, named *Label Assignment Matrix* (*LAM*) (Algorithm 3). To compute *LAM*, first, we associated in the previous frame the set of actively tracked targets $\{T_i^{MOT}\}$ for $i = 1, \dots, M$ to the set of ground truth targets $\{T_i^{GT}\}$ for $i = 1, \dots, M'$, $M \neq M'$ using the Hungarian algorithm and a suitable pairwise distance metric (*pdist*), such as the IoU metric or other, as discussed in the following section:

$$CM = pdist(\{T_i^{MOT}\}_{i=1}^M, \{T_j^{GT}\}_{j=1}^{M'})$$

$$\{(T_{i(k)}^{MOT}, T_{j(k)}^{GT})\}_{k=1}^K = H(CM; T_{assign}) \quad (9)$$

where $CM \in \mathbb{R}^{M \times M'}$ is the pairwise distance matrix, H the Hungarian algorithm.

Next, we enforced a minimum threshold T_{assign} to filter-out the assigned pairs resulting in K pairs. After this step a target T_i^{MOT} can either correspond to a single ground truth target T_j^{GT} ("*on-track*" state) or to none ("*off-track*" state). For "*on-track*" targets we used ground truth box locations since there is a known association, whereas for "*off-track*" we predicted new box locations using the motion model. For the current frame, a $(N \times M)$ pairwise distance matrix is computed between these box locations and the detections using the same metric. Using the *argmax* function we transform each row into a one-hot vector if its max value is over a threshold T_{det2gt} , else we zero-out the whole row. An extra column with zeros is appended to compensate for the non-assignment case resulting in a $(N \times M + 1)$ matrix. Last column elements are set to 1 if all other columns are set to 0 for each row. Finally, each row of the resulting *LAM* matrix is a one-hot vector denoting an association of each detection to a single target (including the *null target* case) and serves as the "label" for the classification problem.

Having computed *LAM* and estimated *ASM* using TADN, we define a categorical cross-entropy loss between them to train our model on. To compensate for the variable number of active targets during training that directly impacts the total categories in the classification problem, we normalized the value of the loss function by dividing with the total number of active targets at each frame. Ultimately, loss function is mean-reduced for all detections:

$$\mathcal{L} = \frac{1}{N \cdot (M + 1)} \cdot \sum_{i=1}^N \sum_{j=1}^M LAM_{i,j} \cdot \log(ASM_{i,j}) \quad (10)$$

After all optimization steps have taken place, we update all targets as described in the previous subsection. However, since this update process is based on the model's predictions, it is expected that in early training stages a lot of erroneous assignments occur due to our model's random initialization. This could lead to an evolving set of targets that wouldn't

Algorithm 2 Target management

Input: Assignments $A_{final} \in \mathbb{R}^N$
 Assignment scores $\{S_i\}_{i=1}^N, S_i \in \mathbb{R}$
 Tracker state: motion and appearance models $\{MM_i, AM_i\}_{i=1}^M$
 Detection locations $\{BB_i\}_{i=1}^N, BB_i \in \mathbb{R}^4$,
 Detection appearance $\{A_i^D\}_{i=1}^N, A_i^D \in \mathbb{R}^{F_D}$

Output: Updated tracker state

Filter-out duplicate assignments :

- 1: $A_{valid} \leftarrow \emptyset$
- 2: **for** each detection $D_i, i = 1, \dots, N$ **do**
- 3: Get assigned target $T_i^{assign} \leftarrow A_{final}[i]$
- 4: **if** (T_i^{assign} is null target) **then**
- 5: $A_{valid} \leftarrow A_{valid} \cup \{(i, T_{null}, -1)\}$
- 6: **else if** (T_i^{assign} not in A_{valid}) **then**
- 7: $A_{valid} \leftarrow A_{valid} \cup \{(i, T_i^{assign}, S_i)\}$
- 8: **else**
- 9: $D_e, S_e \leftarrow A_{valid}[\text{target is } T_i^{assign}]$
- 10: **if** ($S_i > S_e$) **then**
- 11: $A_{valid} \leftarrow A_{valid} - \{(D_e, T_e, S_e)\}$
- 12: $A_{valid} \leftarrow A_{valid} \cup \{(i, T_i^{assign}, S_i)\}$
- 13: **end if**
- 14: **end if**
- 15: **end for**

Update, terminate and spawn targets :

- 16: **for** each target $T_i, i = 1, \dots, M$ **do**
- 17: **if** (T_i in A_{valid}) **then**
- 18: $D_i, S_i \leftarrow A_{valid}[\text{target is } T_i]$
- 19: Update target (MM_i, AM_i)
 using $BB_{D_i}, A_{D_i}^D$
- 20: **else**
- 21: Propagate target state (MM_i, AM_i)
- 22: **end if**
- 23: $T_{h_i} \leftarrow \#$ of hits for T_i
- 24: **if** (T_i # steps unassigned $> T_{h_i}$) **then**
- 25: $T_i \leftarrow$ inactive
- 26: **end if**
- 27: **end for**
- 28: $M' \leftarrow M$
- 29: **for** each detection $D_i, i = 1, \dots, N$ **do**
- 30: **if** ($A_{valid}[D_i]$ contains T_{null}) **then**
- 31: Initialize a new target $k = M' + 1$
 (MM_k, AM_k) using BB_i, A_i^D
- 32: $M' \leftarrow M' + 1$
- 33: **end if**
- 34: **end for**

35: **return** Updated tracker state
 $\{MM_i, AM_i\}_{i=1}^{M'}$

Algorithm 3 LAM computation

Input: Active targets $\{T_i^{MOT}\}, i = 1, \dots, M$
 Ground-truth targets $\{T_i^{GT}\}, i = 1, \dots, M'$
 Detections $\{D_i\}, i = 1, \dots, N$
 Target Assignment threshold T_{assign}
 Detections assignment threshold T_{det2gt}

Output: $LAM \in \mathbb{R}^{N \times M+1}$
 Compute K pairs of active to ground-truth targets :
 1: $\{(T_{i(k)}^{MOT}, T_{j(k)}^{GT})\}_{k=1}^K \leftarrow$ Equation 9
 Classify targets :
 2: $on-track \leftarrow \emptyset$
 3: $off-track \leftarrow \emptyset$
 4: **for** each active target $T_i^{MOT} i = 1, \dots, M$ **do**
 5: **if** $(T_i^{MOT}$ in $\{(T_{i(k)}^{MOT})_{k=1}^K\}$) **then**
 6: $on-track \leftarrow on-track \cup \{T_i^{MOT}\}$
 7: **else**
 8: $off-track \leftarrow off-track \cup \{T_i^{MOT}\}$
 9: **end if**
 10: **end for**
 Compute bbox locations :
 11: Generate $BB_{i=1}^M$ by predicting bbox locations for targets in *off-track* and using GT bbox locations for targets in *on-track*.
 Associate detections to targets :
 12: $LAM \leftarrow pdist(D_{i=1}^N, BB_{j=1}^M)$
 13: $LAM[LAM < T_{det2gt}] \rightarrow 0$
 14: $LAM[LAM \neq \max(LAM, dim = 1)] \rightarrow 0$
 15: $C_1 \leftarrow LAM = \max(LAM, dim = 1)$
 16: $C_2 \leftarrow LAM \neq 0$
 17: $LAM[C_1 \cap C_2] \rightarrow 1$
 Append a column for null target :
 18: $NT \leftarrow \mathbb{0}^{N \times 1}$
 19: $NT[\max(LAM, dim = 1) = 0] \rightarrow 1$
 20: $LAM \leftarrow LAM \oplus NT$
 21: **return** LAM

be representative of a real world tracking problem and could potentially hinder or slow down training. To overcome this, we opted to use LAM to generate assignments instead of the predicted ones. This only affects the latter part of the training step and not the actual optimization procedure. As training epochs progress we used a "choice" probability p_{choice} in order to choose between LAM -generated and TADN-predicted assignment for each detection individually. We gradually altered p_{choice} in favor of our model's prediction using a sigmoid-based transition function relative to elapsed number of epochs. After a certain epoch E_{max} , we used our model's prediction exclusively to step our tracking algorithm:

$$p_{choice}(e) = \sigma\left(-\frac{c}{2} + c \frac{e - E_{min}}{E_{max} - E_{min}}\right) \quad (11)$$

where e the current epoch, σ the sigmoid function, E_{min}, E_{max} the starting and ending epoch for the transition, while c a scaling factor typically set to 12.

4 Experimental Results

We conducted a series of experiments on two well-known datasets, namely MOT17 (Milan et al. [2016]) and UA-DETRAC (Wen et al. [2020]). TADN outperformed all directly comparable methods in many significant metrics, especially delivering superior MOTA performance, thus proving to be a viable alternative to typical computationally expensive data association techniques. In this section, first we present the two benchmarks we evaluated our method

on followed by our implementation details. Next, we present our results along with a qualitative analysis including particular cases of interest regarding the strengths and weaknesses of our method. Last, an extensive ablation study follows investigating and comparing the performance of our method for a curated selection of various configurations.

4.1 Datasets and metrics

MOT17. MOT17 dataset is a part of MOTChallenge (Milan et al. [2016]) which is a standard pedestrian tracking benchmark. MOT17 consists of 7 train and 7 test video sequences depicting stationary and moving pedestrians on a variety of scene configurations varying in camera movement, point of views, occlusions, lighting conditions and video resolutions. All these variations pose a significant challenge for multiple object tracking thus increasing its popularity for measuring the performance for such algorithms. This dataset provides a public detection track provided by three detection algorithms, i.e. Faster-RCNN (Ren et al. [2015]), DPM (Felzenszwalb et al. [2010]) and SDP (Yang et al. [2016b]). To this end, MOT17 distinguishes the performance of MOT algorithms between those exploiting public detections or private detections on a separate track.

For evaluation purposes this benchmark utilizes CLEAR metrics (Bernardin and Stiefelhagen [2008]). MOTA metric combines three error ratios, i.e. false positives, identity switches and missed targets, to intuitively measure accuracy and is considered among the most important metrics for evaluating the performance of a MOT algorithm. On the other hand, MOTP highlights the ability of an algorithm to estimate precise object locations, while IDF1 shows a measure of how many detections are correctly identified. Also, CLEAR metrics provide a thorough insight on how many times a trajectory is fragmented (Frag), how many trajectories are covered by a track hypothesis for their life span (MT, ML) and the total number of missed targets (FN) and identity switches (IDSW).

UA-DETRAC. The UA-DETRAC challenge (Wen et al. [2020]), Lyu et al. [2018], Lyu et al. [2017]) is a vehicle tracking benchmark that includes a mixture of different traffic, weather and illumination conditions from real-world traffic scenes. This benchmark consists of 60 train sequences and 40 test sequences with rich annotations and contains fixed-size sequences (960 x 540) that are recorded at 25 fps with a static camera configuration. Due to its large size and variety of traffic conditions, UA-DETRAC is in fact a very challenging dataset suitable for demonstrating the performance of state-of-the-art MOT algorithms. The benchmark provides a set of public detections from CompACT (Cai et al. [2015]), DPM (Felzenszwalb et al. [2010]), R-CNN (Girshick et al. [2014]) and ACF (Dollár et al. [2014]), while detections from the benchmark’s detection track are also publicly available such as EB (Wang et al. [2017]).

In order to consider both detection and tracking during evaluation, this challenge expands upon CLEAR metrics using the Precision-Recall (PR) curve that is generated by gradually altering the threshold referring to the confidence of the prediction by the object detector. The average of each metric from these series of results for different threshold values is computed, thus introducing the official evaluation metrics of UA-DETRAC, namely PR-MOTA, PR-MOTP, PR-MT, PR-ML, PR-IDSW, PR-FN and PR-FP. It is clear that these metrics are not the most suitable to evaluate our method due to their strong dependency on the selected detector. To mitigate this and provide a detector agnostic performance measure, the maximum MOTA attained was also reported.

4.2 Implementation details

We trained our model on the full MOT17 train set for 300 epochs using a learning rate of $1e^{-4}$ with a step learning rate scheduler that decreased the learning rate value by a factor of 0.1 after 180 epochs. For UA-DETRAC we trained our model on the full train set for 24 epochs and decreased the learning rate after 15 epochs. On either case we set $T_h^{min} = 3$, $T_h^{max} = 30$, $H_{max} = 100$ and we used Adam optimizer (Kingma and Ba [2014]). For MOT17 we used $E_{min} = 20$, $E_{max} = 160$ and for UA-DETRAC $E_{min} = 2$, $E_{max} = 10$. For both datasets we chose to filter-out any detections that have confidence less than 0.3, while also we normalized the bounding box coordinates relative relative to the corresponding image size. We opted for a batch size of 64. It is important to note that our training strategy processes each sample sequentially due to tracking information that need to be updated and propagated across each consecutive sample. Thus, to update our network’s parameters during training we opted for gradient accumulation techniques to form a mini-batch.

Regarding the architectural hyperparameters, we opted for a dual branch TADN module with 2 encoder and decoder layers with 2 heads for each attention layer exploiting both positional and appearance features. We set $d_{model} = 128$, where 64 correspond to positional L_{pos} and 64 to appearance features L_{app} . We used a MOT17 trained reid ResNet50 (He et al. [2016]) as a feature extractor and a CMC-enabled Kalman motion model for both datasets. For all sequences of MOT17 and UA-DETRAC datasets, camera motion compensation (CMC) features were computed using the ECC algorithm introduced by Evangelidis and Psarakis [2008] to compensate for sudden camera motion changes present in some sequences.

We used the publicly available detections from the SDP detector (Yang et al. [2016b]) to train our models for MOT17 and detections produced from the EB (Wang et al. [2017]) detector for UA-DETRAC. Our method was trained and evaluated on a machine with Ryzen 9 3900X 12 core @3.7GHz CPU, a Nvidia 2080Ti GPU and 64GB RAM. The proposed approach was implemented on Pytorch.

As an assignment metric during training time, we opted not to use the Intersection over Union (IoU) metric that is commonly used in such scenarios since it has a constant zero value in cases where two bounding boxes do not overlap. Also, its value alternates in a non-linear fashion for changes in the relative positions between bounding boxes. In the early training stages, it is expected of the predicted bounding boxes to have a significant offset from the ground truth boxes, thus the behavior of the IoU metric could produce false or non-assignments for our model to train on yielding worse performance and slowing down the training process. To mitigate this we introduced a custom assignment metric, namely *upper-left bottom-right* L_1 ($ulbr_1$):

$$ulbr_1(bb_i, bb_j) = - \left| \frac{\|ul_i - ul_j\|_1 + \|br_i - br_j\|_1}{\|ul_i - br_j\|_1 - \|br_i - ul_j\|_1} \right| \quad (12)$$

where $bb_k = [ul_k, br_k] = [x_{min}^k, y_{min}^k, x_{max}^k, y_{max}^k]$.

As discussed in following sections, $ulbr_1$ due to its behaviour to smoothly transition its value even for non-overlapping boxes proves to be a more suitable metric compared to IoU for determining detections to targets assignments during training. For our experiments, we opted for $T_{tgt2det} = -0.13$ using $ulbr_1$ as the assignment metric of choice.

4.3 Evaluation on Benchmarks

TADN was evaluated on the public detections track of MOT17 benchmark against similar state-of-the-art approaches (Table 1). It is worth mentioning that TADN can not be directly compared in a fair way with many popular methods in this benchmark such as TransMOT (Chu et al. [2021]), TransCenter (Xu et al. [2021]), TransTrack (Sun et al. [2020]) or ByteTrack (Zhang et al. [2021]) for a variety of reasons. At first, all these trackers follow a joint detection and tracking paradigm, meaning that they actually employ private detections and not directly use the publicly provided ones. Common techniques employed by most of them to compete in the public detections track are either to impose overlap constraints for target initialization based on the public detections, such as in the work of Zhang et al. [2021], or to limit the maximum number of birth candidates at each frame to the number of public detections available (Xu et al. [2021]). Furthermore, to achieve high performance compared to state-of-the-art many methods use external datasets during training additionally to MOT17 train set, such as CrowdHuman (Shao et al. [2018]) in (Meinhardt et al. [2022]) or HiEve (Lin et al. [2020]) in (Chu et al. [2021]).

Our work is heavily focused on the data association part of a typical MOT pipeline, while in the meantime, the rest consists of rather standard choices (appearance model, motion model). Thus, for a fair comparison, we opted to compare against proven and well established methods that (a) compete in the public detections track following a tracking-by-detection paradigm, (b) use exclusively the data provided by the benchmark and (c) represent a variety of different data association methods. Methods considered are officially published and peer-reviewed in the MOTChallenge benchmark. Quantitative evaluation is based on CLEAR metrics (Bernardin and Stiefelhagen [2008]) which provide a global tracking performance measures such as MOTA and IDF1, as well as a series of more granular metrics regarding important aspects of tracking procedures, such as fragmentation of trajectories (Frag) and identity switches of targets (IDSW).

TADN outperformed all comparable methods regarding MOTA, Mostly Tracked (MT), Mostly Lost (ML), False Negative (FN) metrics while yielding highly competitive performance for IDF1. The results of our simple tracking algorithm prove that TADN can provide a state-of-the-art associative performance for matching targets to detections that can substitute more traditional data association techniques. On the other hand, our method was more sensitive to False Positives (FP), ID Switches (IDSW) and Frag metrics. High FP values denote a frequent drift of a target relative to the ground-truth. This behaviour is mostly due to the simplistic motion model used that fails to predict accurate future locations for the targets. That also leads in a straightforward manner into high Frag values. This phenomenon is also enlarged due to the design of "set-inactive" threshold T_h where targets with few detections can more easily be set to inactive leading to a frequent spawn of new trajectories. Constantly spawning new targets leads to high IDSW values since each ground-truth trajectory is assigned to a series of smaller tracks created by our method. Furthermore, the fact that we did not employ any re-identification module for target "re-birth" or occlusion handling techniques along with the frame-by-frame training strategy formulation have a negative impact on those aforementioned metrics.

In order to study whether our method could generalize into a slightly different tracking benchmark, we tested TADN's performance on the UA-DETRAC dataset (Table 2). Using the EB (Wang et al. [2017]) detector, our proposed method

Table 1: MOT17 results on public detections.

Tracker	DA	MOTA \uparrow	IDF1 \uparrow	MT \uparrow	ML \downarrow	FP \downarrow	FN \downarrow	IDSW \downarrow	Frag \downarrow	Hiz \uparrow
DASOT (Chu et al. [2020])	LA	48.0	51.3	19.9	34.9	38830	250533	3909	-	9.1
DeepMOT (Xu et al. [2020])	e2e-LA	48.1	43.0	17.6	38.6	26490	262578	3696	5353	4.9
DMAN (Zhu et al. [2018])	LA	48.2	55.7	19.3	38.3	26218	263608	2194	5378	0.3
TL-MHT (Sheng et al. [2018a])	MHT	50.6	56.5	17.6	43.4	22213	255030	1407	2079	-
MHT-DAM (Kim et al. [2015])	MHT	50.7	47.2	20.8	36.9	22875	252889	2314	2865	0.9
FAMNet (Chu and Ling [2019])	e2e-MDAP	52.0	48.7	19.1	33.4	14138	253616	3072	5318	<0.1
DAN (Sun et al. [2019])	e2e-LA	52.4	49.5	21.4	30.7	25423	234592	8491	14797	6.3
Tracker (Bergmann et al. [2019])	LA	53.5	52.3	19.5	36.6	12201	248047	2072	4611	1.5
TADN (Ours)	TADN	54.6	49.0	22.4	30.2	36285	214857	4869	7821	10.0

Table 2: UA-DETRAC results.

Detector & Tracker	DA	MOTA \uparrow	MT \uparrow	MOTP \uparrow	ML \downarrow	FP \downarrow	FN \downarrow	IDSW \downarrow
CompACT ² + H2T (Wen et al. [2014])	UHRH	12.4	14.8	35.7	19.4	51765	173899	852
CompACT ² + CMOT (Bae and Yoon [2014])	LA	12.6	16.1	36.1	18.6	57885	167110	285
CompACT ² + GOG (Pirsiavash et al. [2011])	minCF	14.2	13.9	37.0	19.9	32092	180183	3334
EB ³ + IOUT (Bochinski et al. [2017])	LA	19.4	17.7	28.9	18.4	14796	171805	2311
CompACT ² + FAMNet (Chu and Ling [2019])	e2e-MDAP	19.8	17.1	36.7	18.2	14989	164433	617
EB ³ + DAN (Sun et al. [2019])	e2e-LA	20.2	14.5	26.3	18.1	9747	135978	518
EB ³ + Kalman-IOUT (Bochinski et al. [2017])	LA	21.1	21.9	28.6	17.6	19046	159178	462
EB³ + TADN (Ours)	TADN	23.7	61.2	83.2	8.2	31417	198714	2910

^aCLEAR metrics along the detector's PR-curve. Each metric value is the mean value for 10 equally spaced detection thresholds.

²Cai et al. [2015], ³Wang et al. [2017].

DA denotes the employed Data Association approach, \uparrow and \downarrow symbols indicate higher and lower values are preferred respectively.

Abbreviations. e2e: end-to-end trainable, LA: Linear Association, MDAP: Multi-Dimensional Association Problem, MHT: Multiple Hypothesis Tracking, UHRH: Undirected Hierarchical Relation Hypergraph, minCF: min cost flow network based DA.

outperformed competing algorithms against several metrics, i.e. PR-MOTA, PR-MOTP, PR-MT and PR-ML among a variety of selected trackers. Since these metrics are highly dependent on the detector’s performance, in Figure 3 we observed that for a suitable detection threshold, our novel approach achieved over 35% MOTA. High PR-MOTP values are to be expected from our method due to its trend to create several mini trajectories that span across large segments of the ground-truth trajectories. This can also be observed in the low performance on the PR-FP, PR-FN and PR-IDSW metrics that are heavily correlated to the creation of highly fragmented trajectories since our method was focused on solving a frame-by-frame association problem where no specialized measures for long-term associations are used such as occlusion handling, advanced motion model or re-identification modules, as has also been previously discussed for MOT17.

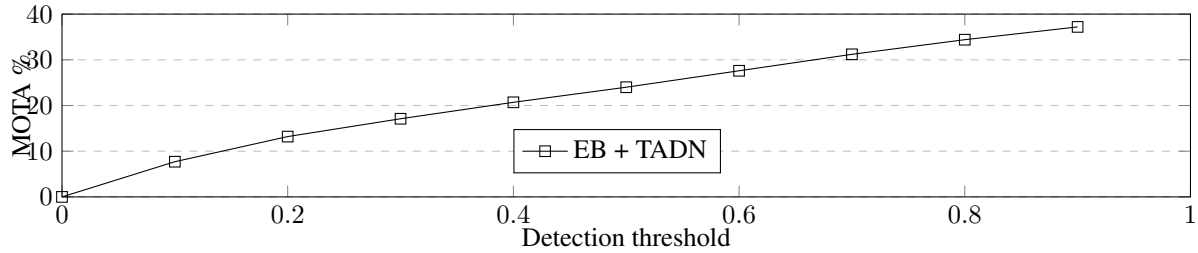


Figure 3: MOTA on UA-DETRAC test set for detection thresholds along the PR-curve.



Figure 4: Success cases from MOT17 test set TADN results in presence of partial occlusion, various scene geometries and illumination conditions. Each pair is ~ 30 frames apart.

Methods that solve a linear assignment problem explicitly which are either end-to-end trainable (Chu and Ling [2019], Xu et al. [2020]) or not (Bergmann et al. [2019], Zhu et al. [2018]) achieve relatively high MOTA values in the cost of inference speed performance. MHT trackers Sheng et al. [2018a] tend to generate less fragmented trajectories with high MOTA and IDF1 values, however they add extra computational cost during inference. TADN’s inference speed, including both detection and association, as shown in Table 1 was significantly higher compared to all other methods and actually only bound to the appearance model inference performance since TADN has a much smaller computational overhead, yielding about 100Hz for the association part. This renders our DA alternative methodology suitable for deployment even on embedded devices to provide real-time tracking.

Qualitatively, we showcase in Figure 4 that in most cases, regarding the MOT17 dataset, our method successfully reconstructs ground truth trajectories. The associative performance of our method seems to be robust even in highly crowded scenes with different camera configurations regarding resolution, scene geometry or illumination conditions. Robustness in target scale changes and partial occlusions demonstrate our model’s capacity to associate positional and appearance features between detections and existing trajectories in the scene. Similar behavior was observed on UA-DETRAC qualitative results as shown on the left pair of images in Figure 6.



Figure 5: Failure examples from MOT17 test set TADN results in presence of poor detections and strong occlusions. Cyan lines: id-switches. Red ellipses: Falsely tracked objects.

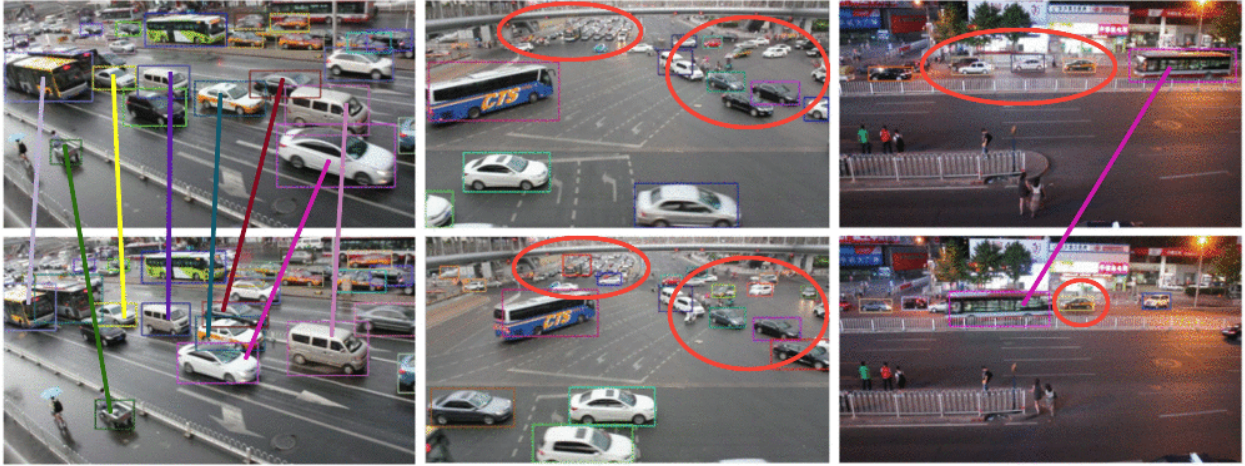


Figure 6: UA-DETRAC test set TADN results. Each pair is ~ 40 frames apart. Left: Success cases with partial occlusions. Mid, Right: Failure cases due to large occlusions, diverse motion dynamics and lack of detections depicted by red colored ellipses.

On the other hand, mostly due to the employed rather simple MOT framework lacking any occlusion handling or re-identification modules produced some failure cases, as shown in Figure 5. In detail, there were some identity switch occurrences where two targets in close proximity had a very similar appearance like the middle example of Figure 5. Also, some tracking errors correlated mostly with false detections provided by the MOT17 benchmark such as those on the first example in Figure 5 where some pedestrians' reflectances were detected consistently and thus tracked by our algorithm. Despite using CMC features, sequences characterized by a moving camera in general tended to perform worse than those with a static camera configuration. Furthermore, our motion model failed to reliably predict future target locations in cases where targets move in complex paths on a crowded scene generating a lot of full occlusions.

Similar problems were also highlighted on UA-DETRAC qualitative results in Figure 6. Here, there were more straightforward cases of total occlusions and highly different motion dynamics for each vehicle in the scene. In either case, our method consistently failed to sustain long-term trajectories and many identity switches occur. Overall, for both datasets, we observed that most errors can be traced back to either false or missing detections or to the simplicity of specific submodules for our MOT approach such as the motion and appearance models used. However, in this work we focused on the frame-by-frame associative performance of our model that is only indirectly linked to such cases.

Table 3: TADN architecture experiments

Architecture parameters						
Heads	Encoder Layers	Decoder Layers	MOTA \uparrow	IDSW \downarrow	FP \downarrow	FN \downarrow
2	2	2	62.2	454	2021	17969
4	2	2	61.5	472	2060	18273
2	4	4	60.6	598	2485	18221
4	4	4	61.0	605	2545	18223
2	2	4	60.8	522	2383	18296

Table 4: Ablation on MOT configuration options

Configuration options					MOTA \uparrow	IDSW \downarrow	FP \downarrow	FN \downarrow
B	F	M.M.	CMC	M				
D	A,P	Kalman	✓	ulbr1	62.2	454	2021	17969
D	A,P	Linear	-	ulbr1	60.2	642	2140	18683
D	A,P	Kalman	-	ulbr1	60.7	450	2070	18716
S	A,P	Kalman	✓	ulbr1	61.5	460	2075	18289
D	A,P	Kalman	✓	IoU	60.8	425	2076	18677
D	P	Kalman	✓	ulbr1	47.5	538	1603	27412
D	A	Kalman	✓	ulbr1	61.3	500	2103	18276
T.S.A.*		Kalman	✓	ulbr1	62.9	702	1003	18358

* Training Strategy-only Assignments. Refers to an ideal tracker where the assignments are directly derived from ground-truth data via our proposed training strategy.

Abbreviations: **B:** # Branches, **F:** Selected features, **M.M.:** Motion model, **CMC:** Camera Motion Compensation, **M:** Assignment metric, **D:** Dual branch TADN, **S:** Single branch TADN, **A:** Appearance features, **P:** Positional features

4.4 Ablation study

To achieve optimal performance, our tracker and TADN in particular require finetuning of multiple hyperparameters and examination of several configuration options. To this end, we conducted a thorough two-part ablation study where, firstly, we investigated multiple architecture configurations for the Transformer architecture in TADN module, while in the second part we explored several other options related to our tracking framework. All ablation were conducted on a 50/50 per sequence split of the original MOT17 training data due to limitations of the test server. In order to assess the results, we used 4 crucial CLEAR metrics, namely MOTA, IDSW, FP and FN.

TADN architecture. We conducted a series of experiments altering three principal Transformer parameters, i.e. number of heads for the multi-head attention layers, number of encoder layers and number of decoder layers (Table 3). In all experiments, it is assumed a dual-branch TADN module using both appearance and positional features coupled with a Kalman motion model with ECC-based CMC and the *ulbr₁* metric as the groundtruth assignment metric during training. All configurations achieved a MOTA greater than 60%, while the most performant combination was achieved by the simplest Transformer architecture yielding also the less ID switches, FP and FN. More complicated models seemed to perform worse, however this might be due to insufficient data that led our model to underfit.

MOT configuration options. A series of experiments with different configurations was conducted examining each time (i) motion model selection and CMC benefits (ii) single or dual branch architectures, (iii) assignment metric during training and (iv) selected features fed to the TADN module (Table 4). Overall, our best model proved to be the one with dual branch TADN module using both appearance and positional features coupled with a CMC-enabled Kalman motion model and *ulbr₁* as the assignment metric during training yielding the best MOTA and FN values and near-best IDSW and FP values. This configuration was considered thus the baseline for all experiments.

By employing a linear motion model the overall performance dropped significantly for every metric in comparison to a Kalman motion model. Enabling CMC further reduced FN metric and boosted MOTA metric by 1.5%. Regarding the single branch configuration, it yielded similar performance for IDSW and FP metrics, however it had lower MOTA value by 0.7% and induced more false negatives showing that the dual branch configuration could reconstruct successfully a bigger part of the ground truth trajectories by a significant margin.

Using IoU as the assignment metric during training seemed to perform significantly worse than the proposed $ulbr_1$ metric in all considered metrics. This fact indicates that $ulbr_1$ is more suitable for training such models since it performs better in cases we have minimal or no overlap between ground truth and predicted bounding boxes during training time. Last, in order to measure the importance of either appearance or positional features that are fed to TADN, we observed that by employing only positional features MOTA dropped by 14.7%. However, that configuration yielded the less false positives among all configurations denoting that positional features are very important to generate as less as possible fragmented trajectories. On the other hand, using only appearance features the performance was close to the baseline (lacking a 0,9%). However, this configuration produced more identity switches compared to the one using both appearance and positional features. This was expected since in general two targets may have similar appearance features but can vary significantly in their location in the scene.

The last row in Table 4 refers to a hypothetical tracker where in each step the final assignments were not derived by our model, but from *LAM* using our training strategy. This experiment was indicative of the expected tracking performance especially during the early stages of training. This measurement directly influenced the final trained model but also gave us an estimate of the maximal performance to be expected given this training strategy. We observed that our model reached this theoretical performance for MOTA metric, outperformed it for IDSW and FN, while underperformed for FP.

Last, we conducted a series of sensitivity analysis experiments for different values of $T_{tgt2det}$ for both assignment metrics $ulbr_1$ and *IoU* where we used the aforementioned hypothetical tracker (Figure 7). Comparing these two metrics, while *IoU* was able to achieve a higher overall MOTA score, it was very sensitive to the threshold value selection. In contrast, the proposed $ulbr_1$ consistently yielded MOTA scores greater than 62.5% for a significant interval of possible thresholds. All in all, for the experiments conducted using the *IoU* and $ulbr_1$ metric we set $T_{tgt2det} = 0.3$ and $T_{tgt2det} = -0.13$ respectively that despite not being the one yielding the best MOTA overall, it was the best compromise between attaining a high MOTA score and being restrictive enough regarding box overlaps.

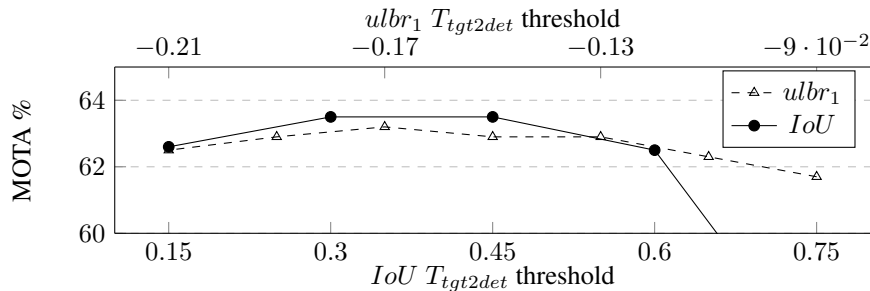


Figure 7: MOTA values for different *IoU* and $ulbr_1$ thresholds. *IoU* achieves better MOTA overall, but is more sensitive to small perturbations.

5 Conclusions

Solving a linear data association problem adds significant computational complexity and in most cases can introduce various problems to multiple object tracking. In this work, we introduced a novel data association method for multiple object tracking via formulating an assignment decision network based on a Transformer architecture. Using our end-to-end training strategy we achieved highly competitive performance compared to state-of-the-art trackers on challenging benchmarks without using any sophisticated submodules referring to appearance or motion modeling.

Overall, TADN demonstrated significant potential in tracking applications, however based on our study it was limited by two factors; our rather simple tracking-by-detection framework employed and our training strategy that derives target associations considering exclusively two consecutive frames. Since during training time ground truth trajectories are available for the whole sequence length, the training strategy could significantly benefit from computing assignments in a non-causal way and potentially yielding better performance especially with metrics related to long-term association performance such as IDSW or Frag. Such a modification does not compromise the online characterization of our approach since it only affects processes during training time, while during testing causality is maintained. Also, using an external detection module has a significant benefit of decoupling the detection from the assignment pipeline hence rendering our approach transferable to new application domains. To improve performance in future work, many state-of-the-art sophisticated modules can be directly incorporated into our tracking pipeline such as occlusion handling, better appearance and motion modelling, more accurate detections and re-identification module.

References

- Wei Tian, Martin Lauer, and Long Chen. Online multi-object tracking using joint domain information in traffic scenarios. *IEEE Transactions on Intelligent Transportation Systems*, 21(1):374–384, 2019.
- Xiaozhi Chen, Huimin Ma, Ji Wan, Bo Li, and Tian Xia. Multi-view 3d object detection network for autonomous driving. In *Proceedings of the IEEE conference on Computer Vision and Pattern Recognition*, pages 1907–1915, 2017a.
- Aljoša Osep, Wolfgang Mehner, Markus Mathias, and Bastian Leibe. Combined image-and world-space tracking in traffic scenes. In *2017 IEEE International Conference on Robotics and Automation (ICRA)*, pages 1988–1995. IEEE, 2017.
- A Psalta, V Tsironis, K Karantzalos, and I Spyropoulou. Social pooling with edge convolutions on local connectivity graphs for human trajectory prediction in crowded scenes. In *2020 IEEE 23rd International Conference on Intelligent Transportation Systems (ITSC)*, pages 1–6, 2020. doi:10.1109/ITSC45102.2020.9294251.
- Yicong Tian, Afshin Dehghan, and Mubarak Shah. On detection, data association and segmentation for multi-target tracking. *IEEE Transactions on Pattern Analysis and Machine Intelligence*, 41(9):2146–2160, 2018.
- Philipp Bergmann, Tim Meinhardt, and Laura Leal-Taixe. Tracking without bells and whistles. In *Proceedings of the IEEE/CVF International Conference on Computer Vision*, pages 941–951, 2019.
- Afshin Dehghan, Yicong Tian, Philip HS Torr, and Mubarak Shah. Target identity-aware network flow for online multiple target tracking. In *Proceedings of the IEEE Conference on Computer Vision and Pattern Recognition*, pages 1146–1154, 2015.
- Harold W Kuhn. The hungarian method for the assignment problem. *Naval Research Logistics Quarterly*, 2(1-2): 83–97, 1955.
- Ashish Vaswani, Noam Shazeer, Niki Parmar, Jakob Uszkoreit, Llion Jones, Aidan N Gomez, Łukasz Kaiser, and Illia Polosukhin. Attention is all you need. *Advances in Neural Information Processing Systems*, 30, 2017.
- Yihong Xu, Aljosa Osep, Yutong Ban, Radu Horaud, Laura Leal-Taixé, and Xavier Alameda-Pineda. How to train your deep multi-object tracker. In *Proceedings of the IEEE/CVF Conference on Computer Vision and Pattern Recognition*, pages 6787–6796, 2020.
- Anton Milan, Laura Leal-Taixé, Ian Reid, Stefan Roth, and Konrad Schindler. Mot16: A benchmark for multi-object tracking. *arXiv preprint arXiv:1603.00831*, 2016.
- Patrick Dendorfer, Aljosa Osep, Anton Milan, Konrad Schindler, Daniel Cremers, Ian Reid, Stefan Roth, and Laura Leal-Taixé. Motchallenge: A benchmark for single-camera multiple target tracking. *International Journal of Computer Vision*, 129(4):845–881, 2021.
- Longyin Wen, Dawei Du, Zhaowei Cai, Zhen Lei, Ming-Ching Chang, Honggang Qi, Jongwoo Lim, Ming-Hsuan Yang, and Siwei Lyu. UA-DETRAC: A new benchmark and protocol for multi-object detection and tracking. *Computer Vision and Image Understanding*, 2020.
- Shaoqing Ren, Kaiming He, Ross Girshick, and Jian Sun. Faster r-cnn: Towards real-time object detection with region proposal networks. *Advances in Neural Information Processing Systems*, 28, 2015.
- Fan Yang, Wongun Choi, and Yuanqing Lin. Exploit all the layers: Fast and accurate cnn object detector with scale dependent pooling and cascaded rejection classifiers. In *Proceedings of the IEEE Conference on Computer Vision and Pattern Recognition*, pages 2129–2137, 2016a.
- Siyu Tang, Bjoern Andres, Mykhaylo Andriluka, and Bernt Schiele. Multi-person tracking by multicut and deep matching. In *Proceedings of the European Conference on Computer Vision*, pages 100–111. Springer, 2016.
- Yifu Zhang, Peize Sun, Yi Jiang, Dongdong Yu, Zehuan Yuan, Ping Luo, Wenyu Liu, and Xinggang Wang. Bytetrack: Multi-object tracking by associating every detection box. *arXiv preprint arXiv:2110.06864*, 2021.
- Alex Bewley, Zongyuan Ge, Lionel Ott, Fabio Ramos, and Ben Upcroft. Simple online and realtime tracking. In *2016 IEEE international conference on image processing (ICIP)*, pages 3464–3468. IEEE, 2016.

- Kuan Fang, Yu Xiang, Xiaocheng Li, and Silvio Savarese. Recurrent autoregressive networks for online multi-object tracking. In *2018 IEEE Winter Conference on Applications of Computer Vision (WACV)*, pages 466–475. IEEE, 2018.
- ShiJie Sun, Naveed Akhtar, HuanSheng Song, Ajmal Mian, and Mubarak Shah. Deep affinity network for multiple object tracking. *IEEE Transactions on Pattern Analysis and Machine Intelligence*, 43(1):104–119, 2019.
- Peng Chu and Haibin Ling. Famnet: Joint learning of feature, affinity and multi-dimensional assignment for online multiple object tracking. In *Proceedings of the IEEE/CVF International Conference on Computer Vision*, pages 6172–6181, 2019.
- Keni Bernardin and Rainer Stiefelhagen. Evaluating multiple object tracking performance: the clear mot metrics. *EURASIP Journal on Image and Video Processing*, 2008:1–10, 2008.
- Donald Reid. An algorithm for tracking multiple targets. *IEEE transactions on Automatic Control*, 24(6):843–854, 1979.
- Jiahui Chen, Hao Sheng, Yang Zhang, and Zhang Xiong. Enhancing detection model for multiple hypothesis tracking. In *Proceedings of the IEEE Conference on Computer Vision and Pattern Recognition Workshops*, pages 18–27, 2017b.
- Hao Sheng, Jiahui Chen, Yang Zhang, Wei Ke, Zhang Xiong, and Jingyi Yu. Iterative multiple hypothesis tracking with tracklet-level association. *IEEE Transactions on Circuits and Systems for Video Technology*, 29(12):3660–3672, 2018a.
- Xinchao Wang, Engin Türetken, Francois Fleuret, and Pascal Fua. Tracking interacting objects using intertwined flows. *IEEE Transactions on Pattern Analysis and Machine Intelligence*, 38(11):2312–2326, 2015.
- Jiawei He, Zehao Huang, Naiyan Wang, and Zhaoxiang Zhang. Learnable graph matching: Incorporating graph partitioning with deep feature learning for multiple object tracking. In *Proceedings of the IEEE Conference on Computer Vision and Pattern Recognition*, pages 5299–5309, 2021.
- Samuel Schulter, Paul Vernaza, Wongun Choi, and Manmohan Chandraker. Deep network flow for multi-object tracking. In *Proceedings of the IEEE Conference on Computer Vision and Pattern Recognition*, pages 6951–6960, 2017.
- Siyu Tang, Mykhaylo Andriluka, Bjoern Andres, and Bernt Schiele. Multiple people tracking by lifted multicut and person re-identification. In *Proceedings of the IEEE Conference on Computer Vision and Pattern Recognition*, pages 3539–3548, 2017.
- Hao Sheng, Yang Zhang, Jiahui Chen, Zhang Xiong, and Jun Zhang. Heterogeneous association graph fusion for target association in multiple object tracking. *IEEE Transactions on Circuits and Systems for Video Technology*, 29(11):3269–3280, 2018b.
- Yu Xiang, Alexandre Alahi, and Silvio Savarese. Learning to track: Online multi-object tracking by decision making. In *Proceedings of the IEEE International Conference on Computer Vision*, pages 4705–4713, 2015.
- Jiawei Liu, Zheng-Jun Zha, Di Chen, Richang Hong, and Meng Wang. Adaptive transfer network for cross-domain person re-identification. In *Proceedings of the IEEE/CVF Conference on Computer Vision and Pattern Recognition*, pages 7202–7211, 2019.
- Nicolas Carion, Francisco Massa, Gabriel Synnaeve, Nicolas Usunier, Alexander Kirillov, and Sergey Zagoruyko. End-to-end object detection with transformers. In *Proceedings of the European Conference on Computer Vision*, pages 213–229. Springer, 2020.
- Tim Meinhardt, Alexander Kirillov, Laura Leal-Taixe, and Christoph Feichtenhofer. Trackformer: Multi-object tracking with transformers. In *Proceedings of the IEEE/CVF Conference on Computer Vision and Pattern Recognition*, pages 8844–8854, 2022.
- Fangao Zeng, Bin Dong, Yuang Zhang, Tiancai Wang, Xiangyu Zhang, and Yichen Wei. Motr: End-to-end multiple-object tracking with transformer. In *Proceedings of the European Conference on Computer Vision*, 2022.
- Peng Chu, Jiang Wang, Quanzeng You, Haibin Ling, and Zicheng Liu. Transmot: Spatial-temporal graph transformer for multiple object tracking. *arXiv preprint arXiv:2104.00194*, 2021.
- Yihong Xu, Yutong Ban, Guillaume Delorme, Chuang Gan, Daniela Rus, and Xavier Alameda-Pineda. Transcenter: Transformers with dense representations for multiple-object tracking. *arXiv preprint arXiv:2103.15145*, 2021.

- Kaiming He, Xiangyu Zhang, Shaoqing Ren, and Jian Sun. Deep residual learning for image recognition. In *Proceedings of the IEEE Conference on Computer Vision and Pattern Recognition*, pages 770–778, 2016.
- Rudolph Emil Kalman. A new approach to linear filtering and prediction problems. *Transactions of the ASME—Journal of Basic Engineering*, 82(Series D):35–45, 1960.
- Georgios D Evangelidis and Emmanouil Z Psarakis. Parametric image alignment using enhanced correlation coefficient maximization. *IEEE Transactions on Pattern Analysis and Machine Intelligence*, 30(10):1858–1865, 2008.
- Pedro F Felzenszwalb, Ross B Girshick, David McAllester, and Deva Ramanan. Object detection with discriminatively trained part-based models. *IEEE Transactions on Pattern Analysis and Machine Intelligence*, 32(9):1627–1645, 2010.
- Fan Yang, Wongun Choi, and Yuanqing Lin. Exploit all the layers: Fast and accurate cnn object detector with scale dependent pooling and cascaded rejection classifiers. In *Proceedings of the IEEE Conference on Computer Vision and Pattern Recognition*, pages 2129–2137, 2016b.
- Siwei Lyu, Ming-Ching Chang, Dawei Du, Wenbo Li, Yi Wei, Marco Del Coco, Pierluigi Carcagni, Arne Schumann, Bharti Munjal, Doo-Hyun Choi, et al. Ua-detrac 2018: Report of avss2018 & iwt4s challenge on advanced traffic monitoring. In *2018 15th IEEE International Conference on Advanced Video and Signal Based Surveillance (AVSS)*, pages 1–6. IEEE, 2018.
- Siwei Lyu, Ming-Ching Chang, Dawei Du, Longyin Wen, Honggang Qi, Yuezun Li, Yi Wei, Lipeng Ke, Tao Hu, Marco Del Coco, et al. Ua-detrac 2017: Report of avss2017 & iwt4s challenge on advanced traffic monitoring. In *2017 14th IEEE International Conference on Advanced Video and Signal Based Surveillance (AVSS)*, pages 1–7. IEEE, 2017.
- Zhaowei Cai, Mohammad Saberian, and Nuno Vasconcelos. Learning complexity-aware cascades for deep pedestrian detection. In *Proceedings of the IEEE International Conference on Computer Vision*, pages 3361–3369, 2015.
- Ross Girshick, Jeff Donahue, Trevor Darrell, and Jitendra Malik. Rich feature hierarchies for accurate object detection and semantic segmentation. In *Proceedings of the IEEE Conference on Computer Vision and Pattern Recognition*, pages 580–587, 2014.
- Piotr Dollár, Ron Appel, Serge Belongie, and Pietro Perona. Fast feature pyramids for object detection. *IEEE Transactions on Pattern Analysis and Machine Intelligence*, 36(8):1532–1545, 2014.
- Li Wang, Yao Lu, Hong Wang, Yingbin Zheng, Hao Ye, and Xiangyang Xue. Evolving boxes for fast vehicle detection. In *2017 IEEE International Conference on Multimedia and Expo (ICME)*, pages 1135–1140. IEEE, 2017.
- Diederik P Kingma and Jimmy Ba. Adam: A method for stochastic optimization. *arXiv preprint arXiv:1412.6980*, 2014.
- Qi Chu, Wanli Ouyang, Bin Liu, Feng Zhu, and Nenghai Yu. Dasot: A unified framework integrating data association and single object tracking for online multi-object tracking. In *Proceedings of the AAAI Conference on Artificial Intelligence*, volume 34, pages 10672–10679, 2020.
- Ji Zhu, Hua Yang, Nian Liu, Minyoung Kim, Wenjun Zhang, and Ming-Hsuan Yang. Online multi-object tracking with dual matching attention networks. In *Proceedings of the European Conference on Computer Vision (ECCV)*, pages 366–382, 2018.
- Chanho Kim, Fuxin Li, Arridhana Ciptadi, and James M Rehg. Multiple hypothesis tracking revisited. In *Proceedings of the IEEE International Conference on Computer Vision*, pages 4696–4704, 2015.
- Longyin Wen, Wenbo Li, Junjie Yan, Zhen Lei, Dong Yi, and Stan Z Li. Multiple target tracking based on undirected hierarchical relation hypergraph. In *Proceedings of the IEEE Conference on Computer Vision and Pattern Recognition*, pages 1282–1289, 2014.
- Seung-Hwan Bae and Kuk-Jin Yoon. Robust online multi-object tracking based on tracklet confidence and online discriminative appearance learning. In *Proceedings of the IEEE Conference on Computer Vision and Pattern Recognition*, pages 1218–1225, 2014.
- Hamed Pirsiavash, Deva Ramanan, and Charless C Fowlkes. Globally-optimal greedy algorithms for tracking a variable number of objects. In *Proceedings of the IEEE Conference on Computer Vision and Pattern Recognition*, pages 1201–1208. IEEE, 2011.

- Erik Bochinski, Volker Eiselein, and Thomas Sikora. High-speed tracking-by-detection without using image information. In *International Workshop on Traffic and Street Surveillance for Safety and Security at IEEE AVSS 2017*, Lecce, Italy, August 2017. URL <http://elvera.nue.tu-berlin.de/files/1517Bochinski2017.pdf>.
- Peize Sun, Jinkun Cao, Yi Jiang, Rufeng Zhang, Enze Xie, Zehuan Yuan, Changhu Wang, and Ping Luo. Transtrack: Multiple object tracking with transformer. *arXiv preprint arXiv:2012.15460*, 2020.
- Shuai Shao, Zijian Zhao, Boxun Li, Tete Xiao, Gang Yu, Xiangyu Zhang, and Jian Sun. Crowddhuman: A benchmark for detecting human in a crowd. *arXiv preprint arXiv:1805.00123*, 2018.
- Weiyao Lin, Huabin Liu, Shizhan Liu, Yuxi Li, Rui Qian, Tao Wang, Ning Xu, Hongkai Xiong, Guo-Jun Qi, and Nicu Sebe. Human in events: A large-scale benchmark for human-centric video analysis in complex events. *arXiv preprint arXiv:2005.04490*, 2020.